Comparative Analysis of Internal Climate Variability and Model Uncertainty on Indian Summer Monsoon Extreme Precipitation

Divya Upadhyay[1], Udit Bhatia[1], and Pranab Mohapatra[1]

[1]Discipline of Civil Engineering, Indian Institute of Technology Gandhinagar, India

Key Points:

- Comparable uncertainty due to internal climate variability to that estimated from multiple model ensembles for precipitation events of disparate duration, frequencies, and extreme volatility for Indian Summer Monsoon Rainfall (ISMR) highlights the inherent challenge to plan for extreme precipitation events.
- Combining outputs from multiple initial condition runs generated to span the range of internal climate variability can help us reduce uncertainty in infrastructure design relevant Depth, Duration and Frequency (DDF) curves.

Corresponding author: Udit Bhatia, bhatia.u@iitgn.ac.in

Abstract

Uncertainty quantification and characterization in changing climate scenarios can have a direct impact on the efforts to mitigate and adapt. Chaotic and non-linear nature of atmospheric processes results in high sensitivity to initial conditions resulting in considerable variability. Multiple model ensembles of Earth System Models are often used to visualize the role of parametric uncertainties in mean and extreme attributes of precipitation trends in various time horizons. However, studies quantifying the role of internal variability in controlling extreme precipitation statistics in decadal and interdecadal scales are limited. In this study, we use a thirty one-member ensemble of Community Earth System Model Large ensemble project and thirty-one ensembles from Coupled Model Intercomparison Project 5 (CMIP5) to quantify the relative contribution of uncertainty due to internal variability in the depth and volatility of Indian Summer Monsoon Rainfall extremes of different durations and frequencies. We find that in the short-term and long-term, the role of internal variability in extreme precipitation indices is comparable to the uncertainty arising from structural differences in the model captured through multiple model ensembles. Further, we show that combining outputs from multiple initial condition runs generated to span the range of internal climate variability can help us reduce uncertainty in infrastructure design relevant Depth Duration and Frequency (DDF) curves.

1 Introduction

Several decades of research and development have undergone to understand the various atmospheric processes and their impact on hydrological processes under the changing climate scenarios at the global scale as well as regional scales (Zhang et al., 2019). Earth System models (ESMs), which are capable of simulating atmospheric processes, are subjected to well-described uncertainties (Asch et al., 2016). However, climate models only provide general information rather than exact information about the future projections of various climate variables, including precipitation and temperature (Schiermeier, 2010). Despite recent advancements in climate model predictions, extreme precipitation is still having higher uncertainty bound. Estimation of return levels of precipitation with less uncertainty is a prerequisite for decision-makers in formulating adaptation policies and economical design of hydraulic structures. There is a need to communicate these uncertainties to the stakeholders (Deser, Knutti, et al., 2012). There are three primary sources of uncertainty in climate projections: that due to future emissions trajectories (characterized through Representative Concentration Pathways or RCP Scenarios), due to Internal Climate Variability (ICV), and due to inter-model differences. While Multiple Model Ensembles can characterize the inter-model differences, Internal Climate Variability is typically handled by considering Multiple Initial Condition Ensembles (MICE) runs. MICE runs are generated by applying minor perturbations to the initial state of the model such that the different climate trajectories are surrogate representations of the natural climate variability (Deser, Knutti, et al., 2012), (Kumar and Ganguly (2018), Stocker et al. (2013), Asch et al. (2016)). On the global scale, Intergovernmental Panel on Climate Change Assessment Report 5 (IPCC AR5) highlights that in the context of global surface temperatures, the RCP scenario spread is the dominant source of uncertainty in the long-term. In contrast, internal variability and inter-model uncertainty dominate in the near term. However, relative contributions of uncertainty at regional and local scales in both mean and extreme attributes of climate variables could be counter-intuitive, calling for regional and local scale analysis.

In the context of the Indian Subcontinent, the Indian Summer Monsoon (ISM) is the major component that provides 80% of the total annual rainfall from June to September (JJAS) in India (Jain & Kumar, 2012). About one-sixth of the world's population affected by the ISM and its variability increased significantly since the 1950s (Goswami

and Chakravorty (2017), Roxy and Chaithra (2018), Ghosh et al. (2016), Ghosh et al. (2012)). Goswami and Xavier (2005) have shown that only about 50% of inter-annual variability of the ISM is explainable, and the remaining part is climate noise. The ISM is a unique tropical climate system with larger spatial as well as temporal variability, which leads to higher uncertainty bounds for the future extreme precipitation, further used for the estimation of the T-year return period flow (RL_T). RL_{30} is useful for most urban drainage system designs (Butler et al., 2018), and RL_{100} and DDF curves are essential for hydraulic engineering designs, operations, and water resources planning or management. Climate adaptation stakeholders require clear guidelines for selecting the value of RL_{30} and RL_{100} with low uncertainty bounds to assimilate climate change effect (Kumar & Ganguly, 2018). Higher uncertainty bound and overlapping of DDF of different year return levels result in lower confidence of decision-makers for adaptation policies and economical design (Alliance (2009), Schindler and Hilborn (2015), Rosenzweig et al. (2011), Hawkins et al. (2014), Deser et al. (2014)). The high variability in ISM extreme precipitation motivated us to further explore the role of ICV as compared to model uncertainty and the effect of concatenation.

Several studies have used ensemble-based approaches to address the internal variability and model uncertainty for prediction of mean and heavy precipitation, temperature and robustness of future changes in local precipitation extremes (Sriver et al. (2015), Kendon et al. (2008), Aalbers et al. (2018), Ghosh and Mujumdar (2007), Ghosh and Mujumdar (2009)). They have also communicated the need to consider numerous Initial Conditions (ICs) and models. The ICV is analysed using 40 member ensembles for precipitation at global scale (Deser, Phillips, et al., 2012) and for US (Deser et al., 2014). Singh and AchutaRao (2019) has considered the CMIP5 and 40-member CESM-LE ensemble for uncertainty analysis for temperature and mean precipitation for India. A recent study shows that the internal variability contributed by the ISM sub-seasonal fluctuations so far considered chaotic is partly predictable (Saha et al., 2019). However, Bhatia and Ganguly (2019) demonstrated that combining multiple ensembles of initial condition runs could help us reduce the parametric (or aleatoric) uncertainty in the estimates of extremes by augmenting the sample size. The concatenation of all ensemble data increases the size of the data for the analysis eventually helps us to reduce the total uncertainty.

In this study, we analyze the role of Internal Climate Variability (ICV) in the projections of extreme precipitation return levels for various duration and frequencies and extreme volatility indices (Fuller et al., 2006) for Indian Summer Monsoon Rainfall (ISMR) using 31 initial condition runs of the same model. We compare the role of ICV in extreme precipitation indices with multiple model ensembles for different time-periods. The Precipitation Extremes Volatility Index (PEVI) and the difference between RL_{100} and RL_{30} in terms of the Inter Quartile Range (IQR) are also analyzed to obtain the measures of uncertainties in design and adaptation relevant indices. Contrary to the findings reported by (Bhatia & Ganguly, 2019), ICV is not only comparable but dominates the uncertainty as obtained from MME for specific regions in India. We also test the applicability of the hypothesis outlined in (Bhatia & Ganguly, 2019), which allows us to concatenate MICE data to reduce the ICV for ISMR. Here, we propose to use multiple models with concatenated multiple initial condition data to envelope total uncertainty. Recently, Deser et al. (2020) provides the opportunity to consider the collection of initial-condition large ensembles (LEs) generated with seven Earth system models under historical and future radiative forcing scenarios. Our study can help scientists and policy-makers to understand and communicate the role of ICV in the context of ISMR, and provide a way to assimilate multiple sources of information to justify actions in climate change adaptation.

2 Data

We obtain observed grid daily precipitation data from the Indian Meteorological Department (IMD) at the resolution of 0.25 degrees (∼25 Square Kilometers) (Pai et al., 2015). To characterize ICV, we obtain 31 IC runs from The National Center for Atmospheric Research (NCAR) Community Earth System Model Large Ensemble Project (LENS). These ICs are obtained by rounding off (order of 10^{-14}°K) differences in air temperature from the single model, and the model is run in coupled mode to obtained projections of state and derived variables including precipitation (Kay et al. (2015), Deser, Phillips, et al. (2012)). To compare the contribution of ICV and model uncertainty in extreme precipitation, we use the output from 31 model ensembles (MME) from the Climate Model Intercomparison Project (CMIP5) for single initial conditions (listed in SI: Table S1). We have used the same number of realizations for MME and MICE to avoid sampling bias. In this study, we have considered extreme Representative Concentration Pathway (RCP 8.5) transient forcing after 2005 for future analysis. However, as more modelling groups produce large ensembles of initial condition runs, this approach can be extended to obtain a clear picture of relative contributions of the uncertainty at regional and local scales.

3 Methodology

To estimate the return level associated with an extreme precipitation event occurring with the probability of a T-year event, we use the Extreme Value Theory (EVT). Specifically, we use the Block Maxima (BM) approach and extract annual maximum precipitation for the period of June-July-August-September (JJAS) from observations, MME, and MICE separately. The details of EVT can be found in (Coles et al., 2001). To match the resolution of models with that of observations, we perform quantile-quantile mapping (Maraun, 2013). We use observed data from the period of 1951 to 2005 for quantile-quantile mapping. To compute the return levels associated with the D-day duration event, we calculate the rolling sum for the number of days under consideration. In the present study, we perform the analysis for 1,2,5,7 and 10 days with return levels of 30-year and 100-year to obtain the Depth-Duration-Frequency curves for ISMR. We calculate The GEV parameters using the Maximum Likelihood Estimate Approach implement through "fevd" and "eva" library of Rpy2 in python to estimate return levels. We report uncertainty in our MLE estimates using 95% confidence intervals. We test for the goodness of fit of the extreme value distributions using the Kolmogorov-Smirnov test at a 5% significance level. We have considered only those points for computation of RL calculation where p-value at grid point greater than 0.05.

For spatial analysis, we consider seven zones of India, as shown in Bhatla et al. (2019) (in SI: Figure S1). Data for four-time windows with different time duration such as 1975-2004 (Historical period), 2006-2035 (Short-term period), 2006-2065 (Medium-term period) and 2006-2095 (Long-term period) are considered separately for RL calculation. RL_{100} and RL_{30} for all grid points over India are calculated independently for MICE and MME. We consider the difference between upper and lower bound as uncertainty measure for individual models for return levels and IQR as the measure for uncertainty within ensembles such as MICE and MME. The temporal variability of RL_{100} is analyzed for historical and RCP 8.5 emission scenario. We consider 30-year moving window and analyze the trend of the average value of an estimated RL_{100} over all grid points in terms of time series (in SI: Figure S2). Time series of historical data shows the similarity between the uncertainty bounds of MICE and MME. In contrast, it indicates higher uncertainty bound and an increasing trend for MICE RCP 8.5. For further investigation, we analyze the ratio of different future duration with historical RL_{100} data (in SI: Figure S3), which also shows the shift towards higher values of RL_{100}. This evidence indicates that ICV is more significant than model uncertainty for ISM extreme precipitation and ignoring ICV results in an underestimation of RL_{100}.

The PEVI, which is the ratio of RLs and also consider a measure of the variability of extreme, is calculated to find the volatility of extreme precipitation (Khan et al., 2007). The rationale in using PEVI is that it can serve as an indicator of the safety factor for infrastructure design. We consider PEVI as the ratio of RL_{100} to RL_{30} by considering that magnitude corresponding to RL_{30} is used for design and RL_{100} is a rarer event. The PEVI takes unity or more than unity value as RL_{30} can not be more than RL_{100}. The unity value represents that magnitude corresponding to both return level are same. Higher PEVI indicates that either only rarer event magnitude or both events quantities are increasing. Thus, to get a more precise idea, we also analyze the difference of both return levels. The decrease in the difference between RL_{100} and RL_{30} indicates that the frequency of rarer extreme events is approaching to design magnitude, which is an alarming situation for the stakeholders.

For extreme precipitation analysis, we consider the annual maximum value for the investigation, which limits the size of the data. MICE data, coming from the same model, allows us to concatenate data. The concatenation approach enables us to augment the sample size of extremes and hence reduce the uncertainty in the estimation of parameters of GEV (Bhatia & Ganguly, 2019). The DDF curves are developed from concatenated MICE data and compare it with the average overall MICE data.

4 Results and discussions

Figure 1 (a) compares the uncertainty in estimates of RL_{100} (daily precipitation) for two randomly selected models from MICE and MME (out of 31 models) as well as among the models for a future period (2006-2035). The supplementary section provides the results for historical, 2006-2065 and 2006-2095 duration in Figure S6, S7 and S8 respectively. The difference between the upper and lower bound of RL_{100} is an indicator of the uncertainty of estimates. Thus, We analyse the difference between bounds for an individual model from MICE and MME for all grids over India. Similarly, IQR of difference between bounds among both MICE and MME are analysed as an indicator of ICV and model uncertainty, which we find comparable for historical data. In contrast, we observe higher uncertainty bounds from a single model and IQR for MICE as compared to MME for 2006-2035 duration. The medium-term (2006-2065) and long-term (2006-2095) data analysis further indicates that uncertainty in the estimation of return levels for many grids over the central part of India is higher for MICE. We observe an increasing trend for uncertainty in the estimate of return levels and ICV. While model uncertainty does not show significant improvement by increasing the duration of the analysis. Higher IQR indicates higher uncertainty so, ignoring it can lead to underestimation as well as a decrease in confidence. The multiplying effect of uncertainties results in larger uncertainty bands for DDF curves which can be ambiguous information for the stakeholders. We observe a similar kind of observation for PEVI and difference of return levels for the same models as shown for RL_{100} (Figure 1 (b-c)). Two randomly selected MICE shows higher PEVI values for the western and northern part of India as compared to MME. The difference between RLs also exhibits similar behaviour. Higher IQR in return levels, PEVI and difference between return levels among MICE indicates that ignoring ICV leads to underestimation of result.

We perform uncertainty analysis to understand the spatial variability by dividing India into seven different zones. The uncertainty/IQR of RL_{100} estimated from a single model of MICE (IC1) and MME. The uncertainty/IQR of IQR values in RL_{100} from 31 ensembles of MICE/MME are compared for each zone (Figure 2). Results of uncertainty bounds for MICE and MME are comparable for all zones except zone 3 and 4 for the historical data. (Figure 2 (a)). For the future period, IQR for single model indicates increase in MICE for all the zones except zone 7 (Figure 2 (b)) and IQR among 31 ensembles of MICE is significantly higher with increased upper bound which indicates the importance of ICV as compared to model uncertainty.

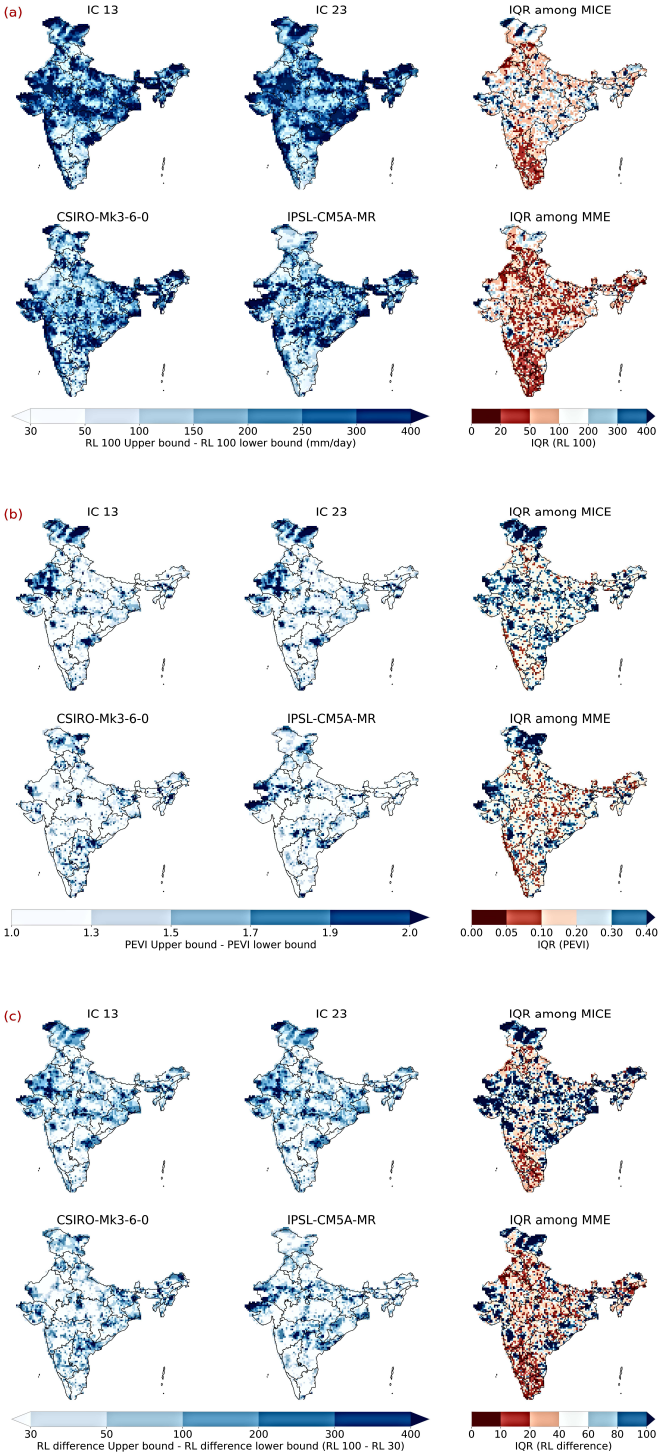

Figure 1. ICV resulting from different ICs is comparable to model uncertainties and even higher in some cases. In **(a)**, First raw shows the RL_{100} for all grids over India for two randomly selected runs from MICE and IQR among 31 MICE and second raw shows RL_{100} for all grids over India for two randomly selected runs from MME and IQR among 31 MME. **(b - c)** shows the results for PEVI and RL difference, respectively. These results for 2006−2035 demonstrate the spatial variability and also among the different model variability for India. (similar results for the historical period, 2006−2065 and 2006−2095 are shown in SI: Figure S6, S7, and S8 respectively)

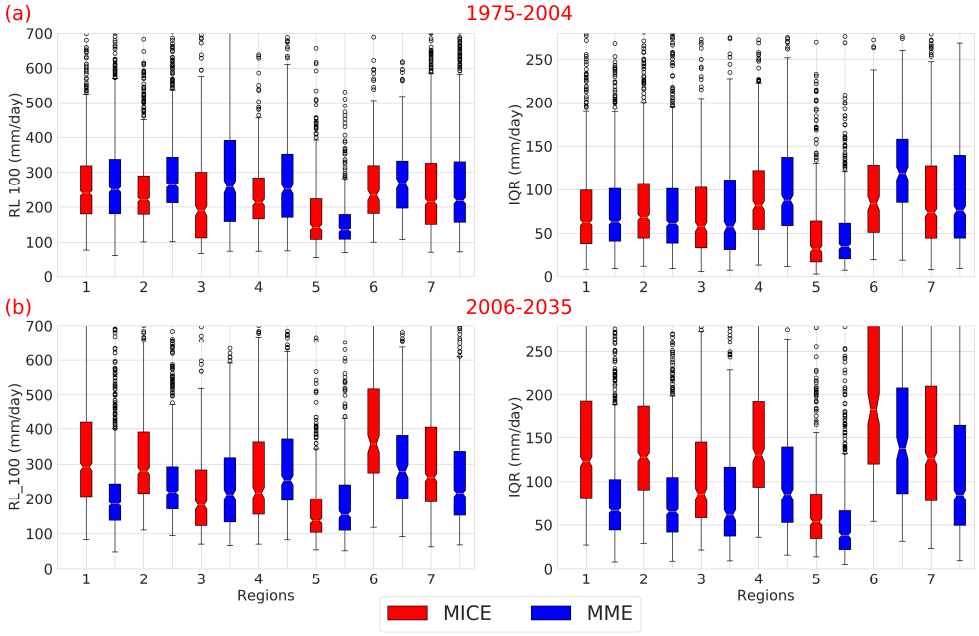

Figure 2. IQR for RL_{100} of single realization (spatial variability) and IQR among the 31 models (realization uncertainty) for all seven zones shows significant variability for the future period, especially for MICE. **(a)** shows IQR for spatial daily RL_{100} for randomly selected single model form MICE and MME and the second figure shows the IQR for IQR among the 31 models for the historical period (1975−2004) indicating that uncertainty of MICE is comparable with MME. **(b)** shows similar results for a future period (2006−2035) indicating that MICE shows the higher uncertainty in RL_{100} as well as for IQR and also shows higher upper bounds for all regions. The figure shows numerous outliers even above this limit (not shown here), indicates that the number of models is required for better understanding.

Bhatia and Ganguly (2019) have shown more substantial variability in MME but significantly higher upper bounds from MICE for US hydro-meteorological zones. However, higher uncertainty, as well as significantly higher upper limits in RL_{100}, are observed from MICE for ISM extreme precipitation for all zones of India.

Figure 3 validates of the hypothesis related to the concatenation of MICE. Average uncertainties (upper bound - lower bound) in RL_{100} for all 31 ICs (Figure 3 (a)) are significantly higher for most of the grid points. Uncertainties from concatenated all 31 ICs indicates significant reduction for almost all grid points (Figure 3 (b)). The distribution of the mean, upper bound and lower bound of estimated RL_{100} average over each zone also gives a clear indication of improvement in uncertainty reduction and the effect of concatenation (Figure 3 (c - d)). Mean of concatenated data also gives agreement with observed data (3 (c)) indicating that it is trying to capture observation behaviour more precisely.

The effect of data duration considered for the analysis are shown in Figure 4. This figure indicates return level average over a specific zone. The DDF curves for RL_{100} and RL_{30} with upper and lower bound (uncertainty bounds) with a 95 % confidence level for randomly selected three zones shows the effect of duration of the analysis. Uncertainty bounds of RL_{30} coincide with bound of RL_{100} for all the periods, which imparts diffi-

culty in selecting appropriate precipitation intensity for the design, maintenance and operations of hydraulic infrastructure and for water resources planning and management. The 2006-2035 period shows the highest uncertainty as compared to other duration. For medium-term duration to long-term duration data, there is a decrease in uncertainty bounds with overlapping of both DDF curves.

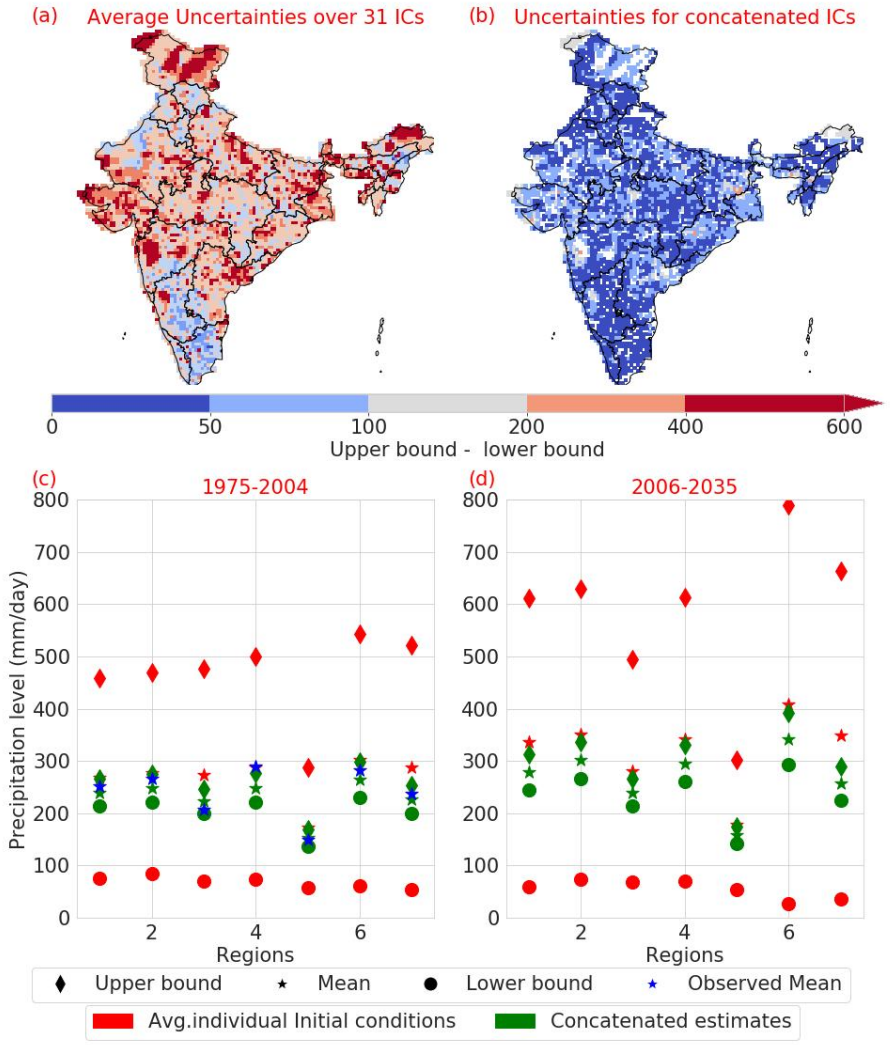

Figure 3. The validation of reduction in uncertainty due to concatenation of the data from the 31 MICE is shown. **(a - b)** shows the average uncertainties (upper bound - lower bound) over 31 MICE data and compared with the uncertainties of concatenated data for historical data for each grid. **(c - d)** shows the uncertainty bounds for average over 31 MICE (red) and for concatenated data (green) for each zone and compared it with observation (blue) for historical data **(c)**.

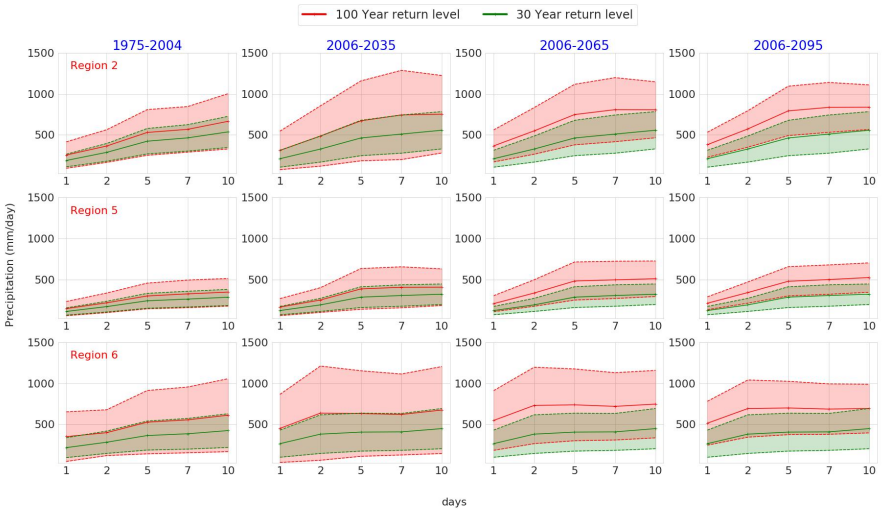

Figure 4. The DDF curves developed using for different period data (1975−2004, 2006−2035, 2006−2065, 2006−2095) for 3 randomly selected zones out of 7 zones of India for RL_{100} and RL_{30} with upper and lower bounds are shown. (curves for 7 zones are shown in SI: fig S4).

The effect of the concatenation of MICE in the form of DDF curves for randomly selected three zones out of seven is shown in Figure 5. The uncertainty bounds of RL_{100} and RL_{30} becomes narrower and significantly distinguished from each other as a result of concatenation, which can be more useful and valuable for the stakeholders for taking decisions.

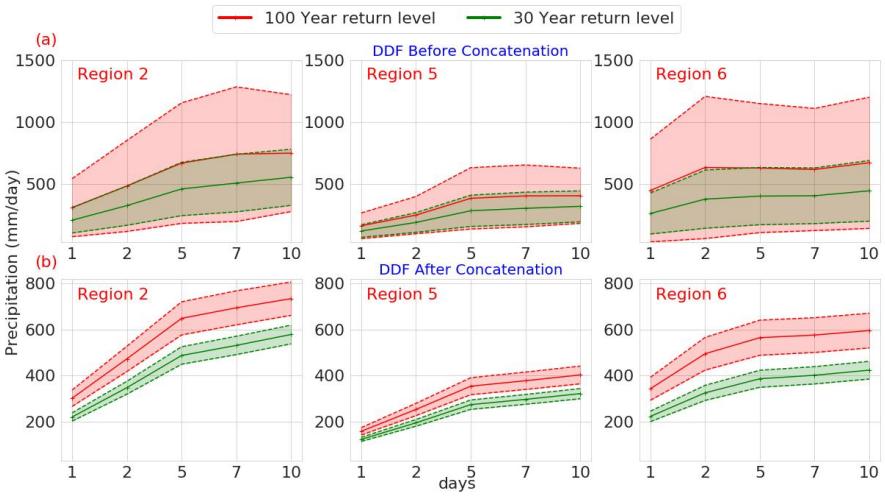

Figure 5. The DDF curves for future data (2006−2035) for randomly selected 3 zones are shown. The first raw **(a)** provides the estimated DDF average over particular zonal grids with upper and lower bound for RL_{100} and RL_{30} for IC1 model before concatenation. The second raw **(b)** shows the results for zonal average estimates results after concatenation of all 31 MICE data.(The DDF curves generated from concatenated 31 MICE for all 7 zones with all 4 periods are shown in SI, fig S5)

5 Conclusions

We have analyzed the uncertainties in 100-year and 30-year return levels using extreme value theory for ISM precipitation. MME (one initial condition, multiple models) and MICE (one model, various initial conditions) are used to handle model uncertainty and internal climate variability, respectively. These climate models are widely used to forecast extreme rainfall events. We consider 31 MICE and 31 MME, the same number of ensembles to remove the sampling bias. The estimates of RL_{100} from both MICE and MME shows that there is significant spatial variability. The uncertainty bounds estimated using historical data indicate that ICV is comparable with model uncertainty. However, the uncertainty bounds calculated using future data shows an increasing trend with significantly higher uncertainty as compared to model uncertainty. The time series of average return level over 30-years moving window also supports the growing trend. This trend becomes more intense as we consider long-term data (2006-2095). The MICE shows increasing PEVI and difference in RLs, indicating that infrequent and high-intensity events are approaching towards frequent and low-intensity events. The uncertainty among the ensembles for future periods is more prominent for many points in MICE analysis. This CESM-LE (MICE) captures key oscillatory coupled climate patterns, such as the interannual variability in tropical Pacific sea surface temperatures associated with the El Niño Southern Oscillation (ENSO), Pacific decadal variability, Atlantic multidecadal variability, etc. Such events largely influence the ISM extreme precipitation, which results in higher uncertainty. This study reveals that ignoring ICV results in an underestimation of extreme precipitation for the Indian Subcontinent. The uncertainty analysis considers fixed duration data for investigation using historical duration and future periods such as 2006-2035, 2006-2065, and 2006-2095. Thus, the future scope includes the trend analysis for PEVI and the difference in RL values to analyze the severity of RL selection for designing hydraulic structures. RL calculation is computationally expensive, although we have only considered one maximum value, block maxima approach, rather than all the extreme events of the year. However, Generalized Pareto Distribution (GPD) accounts for all the activities above the threshold with a high probability of violating IID assumption, which is considered as a critical assumption. This GPD is out of the scope of this paper. We observed that even using GPD, it does not make a significant difference in RL_{100}. The DDF curves show the considerable overlapping of average estimated RL_{100} and RL_{30} for all seven zones, which can create confusion for the decision-makers. The concatenation of MICE shows a significant reduction in uncertainty bounds. It is also capable of distinguishing the RL_{100} and RL_{30} uncertainty bounds, which is essential information to the stakeholders for making decisions. The results from the concatenated MICE from one model and its comparison with MME recommends using multiple models with concatenated multiple initial condition data. With more and more initial condition ensembles being made available as a part of forthcoming CMIP6 data, there is a need to inform and incorporate the estimates of internal variability to furnish a clear picture for the stakeholders for making essential decisions for mitigation and adaptation.

Acknowledgments

This work was supported by DST-SERB Startup Research grant, and Indian Institute of Technology Gandhinagar Internal Research Grant. High-resolution observations over India were distributed by Indian Meteorological Department located at Pune.

Author Contributions

Udit Bhatia and Divya Upadhyay designed the experiments. Divya Upadhyay performed the experiments and analyzed the data. Udit Bhatia, Divya Upadhyay and Pranab Mohapatra wrote the manuscript.

Data Availability

LENS datasets can be downloaded from http://www.cesm.ucar.edu/projects/community-projects/LENS/. CMIP5 dataset is freely available from https://cmip.llnl.gov/cmip5/data_portal.html.

References

Aalbers, E. E., Lenderink, G., van Meijgaard, E., & van den Hurk, B. J. (2018). Local-scale changes in mean and heavy precipitation in western europe, climate change or internal variability? *Climate Dynamics*, *50*(11-12), 4745–4766.

Alliance, W. U. C. (2009). Options for improving climate modeling to assist water utility planning for climate change. *Avilable at: http://www. wucaonline. org/html.(accessed October 10, 2011)*.

Asch, R. G., Pilcher, D. J., Rivero-Calle, S., & M Holding, J. (2016). Demystifying models: answers to ten common questions that ecologists have about earth system models.

Bhatia, U., & Ganguly, A. R. (2019). Precipitation extremes and depth-duration-frequency under internal climate variability. *Scientific reports*, *9*(1), 1–9.

Bhatla, R., Verma, S., Ghosh, S., & Mall, R. (2019). Performance of regional climate model in simulating indian summer monsoon over indian homogeneous region. *Theoretical and Applied Climatology*, 1–15.

Butler, D., Digman, C. J., Makropoulos, C., & Davies, J. W. (2018). *Urban drainage*. Crc Press.

Coles, S., Bawa, J., Trenner, L., & Dorazio, P. (2001). *An introduction to statistical modeling of extreme values* (Vol. 208). Springer.

Deser, C., Knutti, R., Solomon, S., & Phillips, A. S. (2012). Communication of the role of natural variability in future north american climate. *Nature Climate Change*, *2*(11), 775–779.

Deser, C., Phillips, A., Bourdette, V., & Teng, H. (2012). Uncertainty in climate change projections: the role of internal variability. *Climate dynamics*, *38*(3-4), 527–546.

Deser, C., Phillips, A. S., Alexander, M. A., & Smoliak, B. V. (2014). Projecting north american climate over the next 50 years: Uncertainty due to internal variability. *Journal of Climate*, *27*(6), 2271–2296.

Fuller, C. T., Sabesan, A., Khan, S., Kuhn, G., Ganguly, A. R., Erickson, D., & Ostrouchov, G. (2006). Quantification and visualization of the human impacts of anticipated precipitation extremes in south america. *Eos Transactions, American Geophysical Union*, *87*, 52.

Ghosh, S., Das, D., Kao, S.-C., & Ganguly, A. R. (2012). Lack of uniform trends but increasing spatial variability in observed indian rainfall extremes. *Nature Climate Change*, *2*(2), 86–91.

Ghosh, S., & Mujumdar, P. (2007). Nonparametric methods for modeling gcm and scenario uncertainty in drought assessment. *Water Resources Research*, *43*(7).

Ghosh, S., & Mujumdar, P. (2009). Climate change impact assessment: Uncertainty modeling with imprecise probability. *Journal of Geophysical Research: Atmospheres*, *114*(D18).

Ghosh, S., Vittal, H., Sharma, T., Karmakar, S., Kasiviswanathan, K., Dhanesh, Y., ... Gunthe, S. (2016). Indian summer monsoon rainfall: implications of contrasting trends in the spatial variability of means and extremes. *PloS one*, *11*(7), e0158670.

Goswami, B., & Chakravorty, S. (2017). Dynamics of the indian summer monsoon climate. In *Oxford research encyclopedia of climate science*.

Goswami, B., & Xavier, P. K. (2005). Dynamics of "internal" interannual variability of the indian summer monsoon in a gcm. *Journal of Geophysical Research: Atmospheres*, *110*(D24).

Hawkins, E., Anderson, B., Diffenbaugh, N., Mahlstein, I., Betts, R., Hegerl, G., ... others (2014). Uncertainties in the timing of unprecedented climates. *Nature*, *511*(7507), E3–E5.

Jain, S. K., & Kumar, V. (2012). Trend analysis of rainfall and temperature data for india. *Current Science*, 37–49.

Kay, J. E., Deser, C., Phillips, A., Mai, A., Hannay, C., Strand, G., ... others (2015). The community earth system model (cesm) large ensemble project: A community resource for studying climate change in the presence of internal climate variability. *Bulletin of the American Meteorological Society*, *96*(8), 1333–1349.

Kendon, E. J., Rowell, D. P., Jones, R. G., & Buonomo, E. (2008). Robustness of future changes in local precipitation extremes. *Journal of climate*, *21*(17), 4280–4297.

Khan, S., Kuhn, G., Ganguly, A. R., Erickson III, D. J., & Ostrouchov, G. (2007). Spatio-temporal variability of daily and weekly precipitation extremes in south america. *Water Resources Research*, *43*(11).

Kumar, D., & Ganguly, A. R. (2018). Intercomparison of model response and internal variability across climate model ensembles. *Climate dynamics*, *51*(1-2), 207–219.

Maraun, D. (2013). Bias correction, quantile mapping, and downscaling: Revisiting the inflation issue. *Journal of Climate*, *26*(6), 2137–2143.

Pai, D., Sridhar, L., Badwaik, M., & Rajeevan, M. (2015). Analysis of the daily rainfall events over india using a new long period (1901–2010) high resolution (0.25× 0.25) gridded rainfall data set. *Climate dynamics*, *45*(3-4), 755–776.

Rosenzweig, C., Solecki, W. D., Blake, R., Bowman, M., Faris, C., Gornitz, V., ... others (2011). Developing coastal adaptation to climate change in the new york city infrastructure-shed: process, approach, tools, and strategies. *Climatic change*, *106*(1), 93–127.

Roxy, M., & Chaithra, S. (2018). *Impacts of climate change on the indian summer monsoon.* Ministry of Environment, Forest and Climate Change (MoEF&CC), Government of ....

Saha, S. K., Hazra, A., Pokhrel, S., Chaudhari, H. S., Sujith, K., Rai, A., ... Goswami, B. (2019). Unraveling the mystery of indian summer monsoon prediction: improved estimate of predictability limit. *Journal of Geophysical Research: Atmospheres*, *124*(4), 1962–1974.

Schiermeier, Q. (2010). The real holes in climate science: like any other field, research on climate change has some fundamental gaps, although not the ones typically claimed by sceptics. quirin schiermeier takes a hard look at some of the biggest problem areas. *Nature*, *463*(7279), 284–288.

Schindler, D. E., & Hilborn, R. (2015). Prediction, precaution, and policy under global change. *Science*, *347*(6225), 953–954.

Singh, R., & AchutaRao, K. (2019). Quantifying uncertainty in twenty-first century climate change over india. *Climate dynamics*, *52*(7-8), 3905–3928.

Sriver, R. L., Forest, C. E., & Keller, K. (2015). Effects of initial conditions uncertainty on regional climate variability: An analysis using a low-resolution cesm ensemble. *Geophysical Research Letters*, *42*(13), 5468–5476.

Stocker, T. F., Qin, D., Plattner, G.-K., Tignor, M., Allen, S. K., Boschung, J., ... others (2013). Climate change 2013: The physical science basis. *Contribution of working group I to the fifth assessment report of the intergovernmental panel on climate change*, *1535*.

Zhang, Y., Li, H., & Reggiani, P. (2019). *Climate variability and climate change impacts on land surface, hydrological processes and water management.* Multidisciplinary Digital Publishing Institute.

Figure_1.pdf.

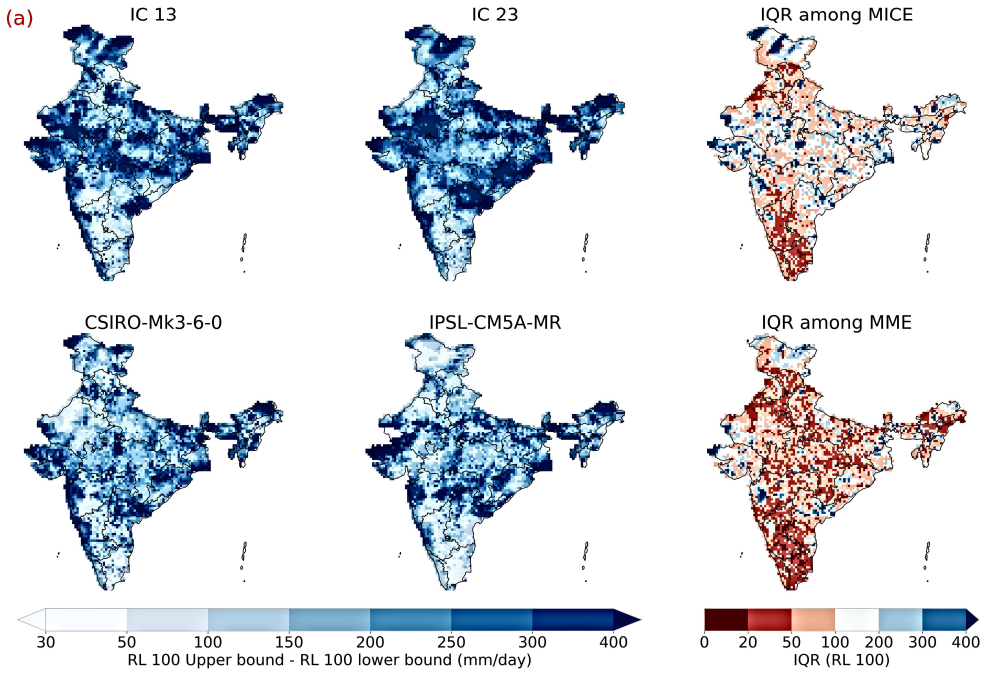
(a)
IC 13
IC 23
IQR among MICE
CSIRO-Mk3-6-0
IPSL-CM5A-MR
IQR among MME
30 50 100 150 200 250 300 400
RL 100 Upper bound - RL 100 lower bound (mm/day)
0 20 50 100 200 300 400
IQR (RL 100)

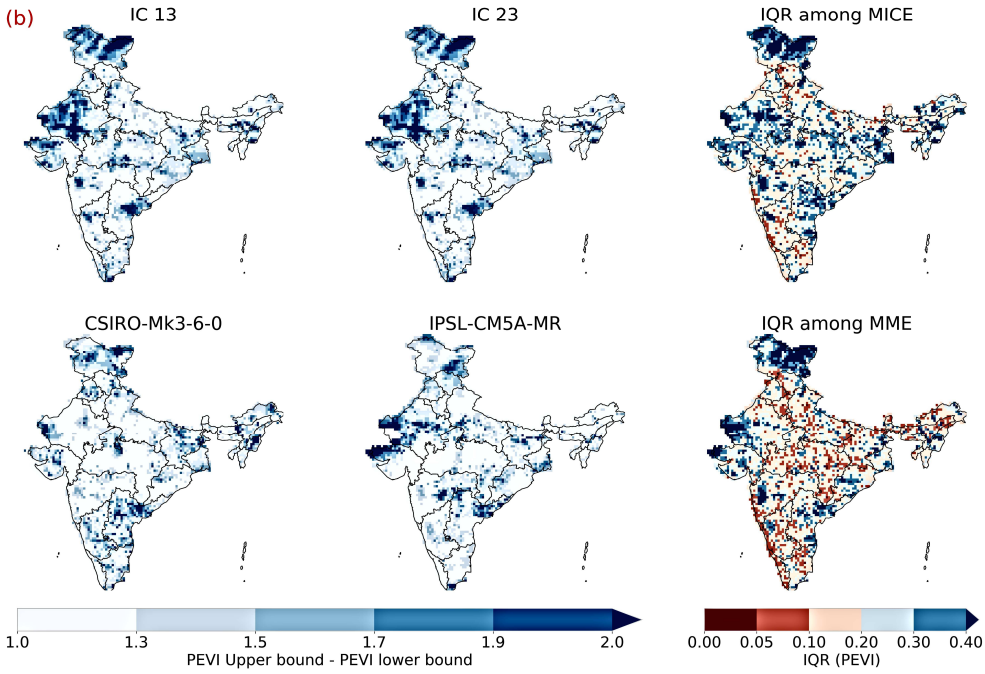
(b)
IC 13
IC 23
IQR among MICE
CSIRO-Mk3-6-0
IPSL-CM5A-MR
IQR among MME
1.0 1.3 1.5 1.7 1.9 2.0
PEVI Upper bound - PEVI lower bound
0.00 0.05 0.10 0.20 0.30 0.40
IQR (PEVI)

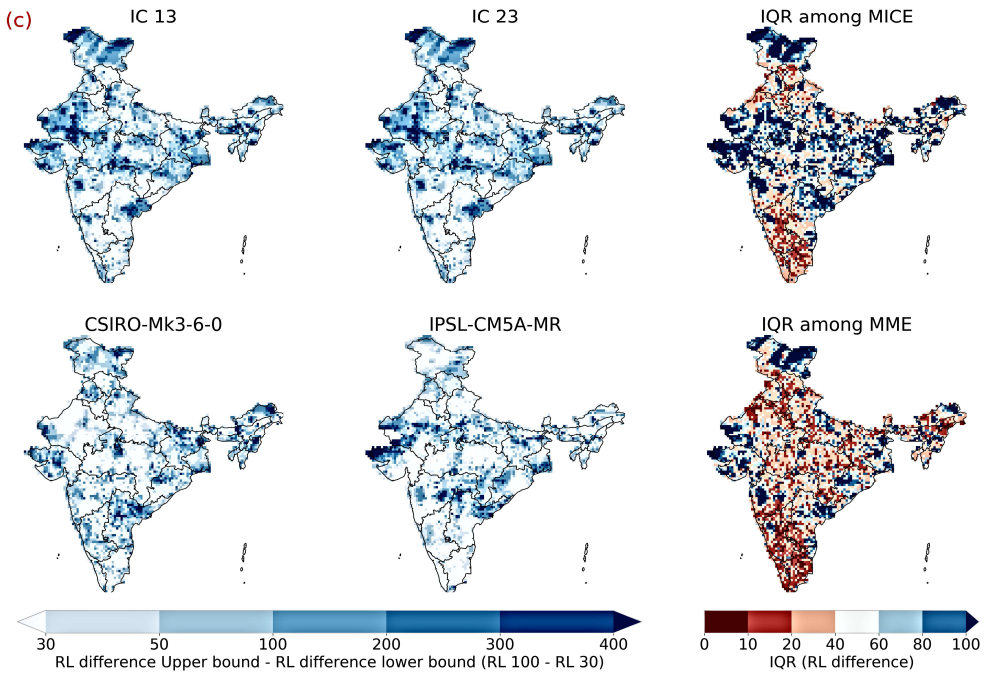
(c)
IC 13
IC 23
IQR among MICE
CSIRO-Mk3-6-0
IPSL-CM5A-MR
IQR among MME
30 50 100 200 300 400
RL difference Upper bound - RL difference lower bound (RL 100 - RL 30)
0 10 20 40 60 80 100
IQR (RL difference)

Figure_2.pdf.

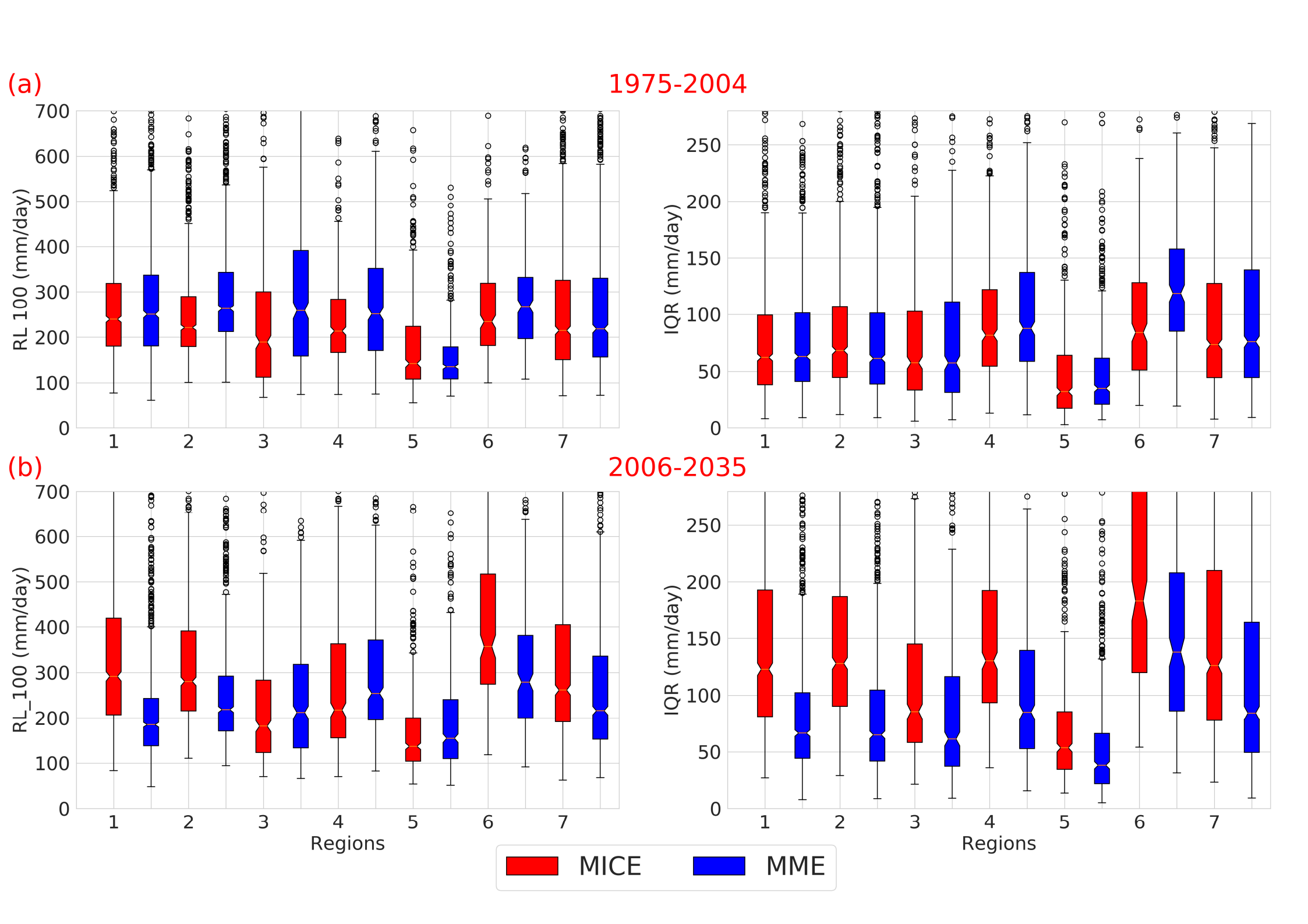
(a)
1975-2004
RL 100 (mm/day)
IQR (mm/day)
(b)
2006-2035
RL_100 (mm/day)
IQR (mm/day)
Regions
Regions
MICE
MME

Figure_3.pdf.

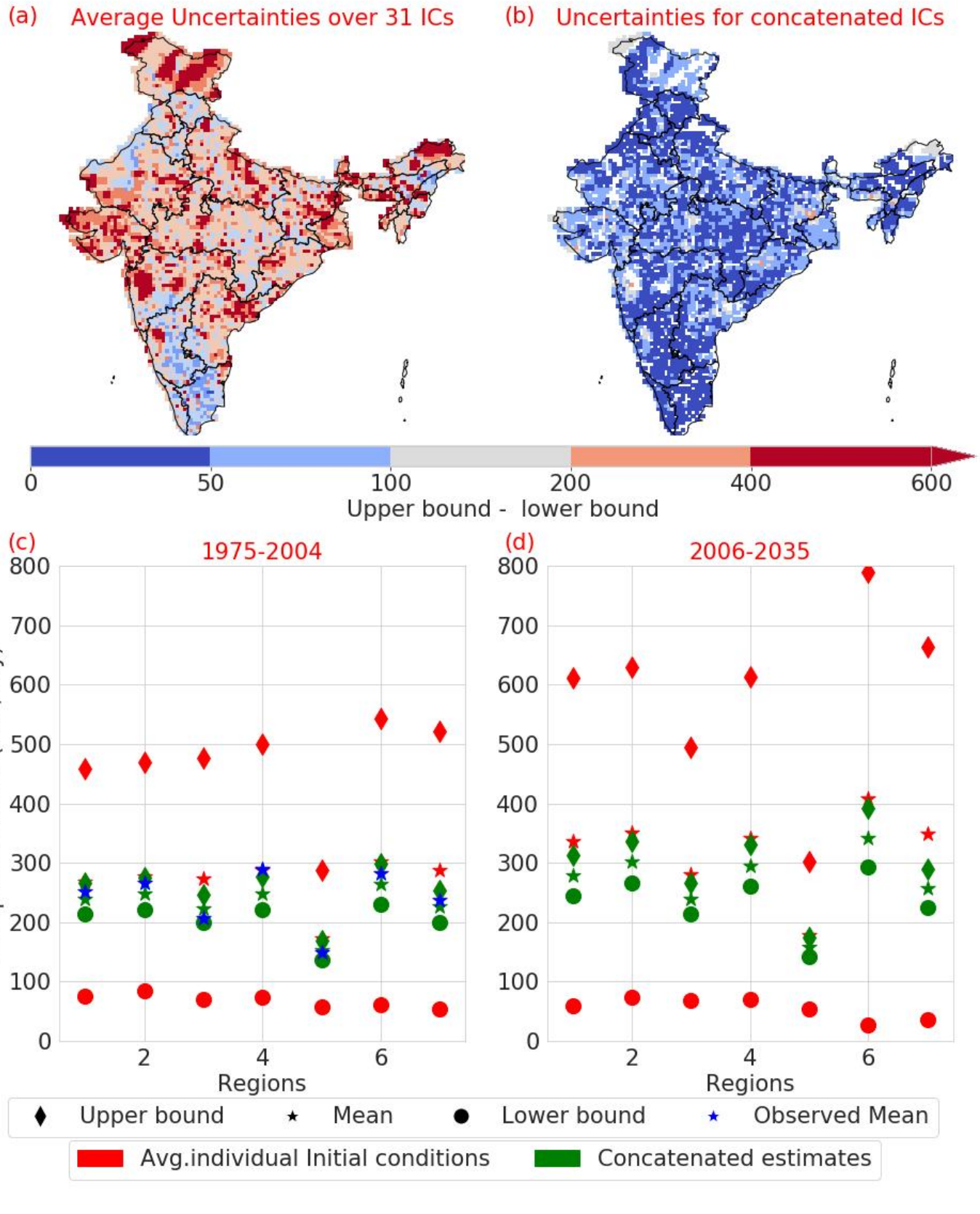
(a) Average Uncertainties over 31 ICs
(b) Uncertainties for concatenated ICs
0
50
100
200
400
600
Upper bound - lower bound
(c) 1975-2004
(d) 2006-2035
Precipitation level (mm/day)
800
700
600
500
400
300
200
100
0
2
4
6
Regions
Upper bound
Mean
Lower bound
Observed Mean
Avg.individual Initial conditions
Concatenated estimates

Figure_4.pdf.

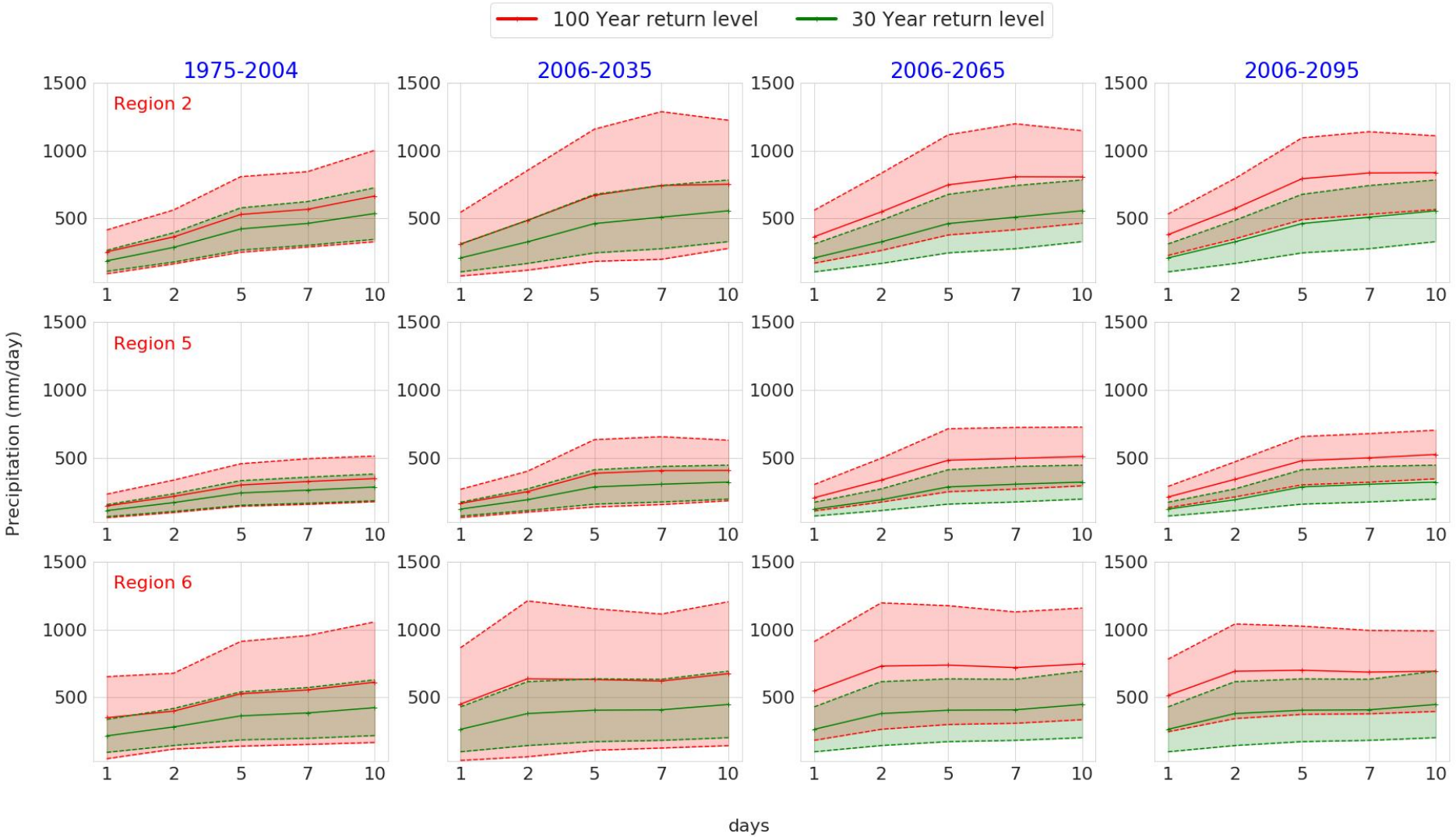
100 Year return level
30 Year return level
1975-2004
2006-2035
2006-2065
2006-2095
Region 2
Region 5
Region 6
Precipitation (mm/day)
days
1500
1000
500
1
2
5
7
10

Figure_5.pdf.

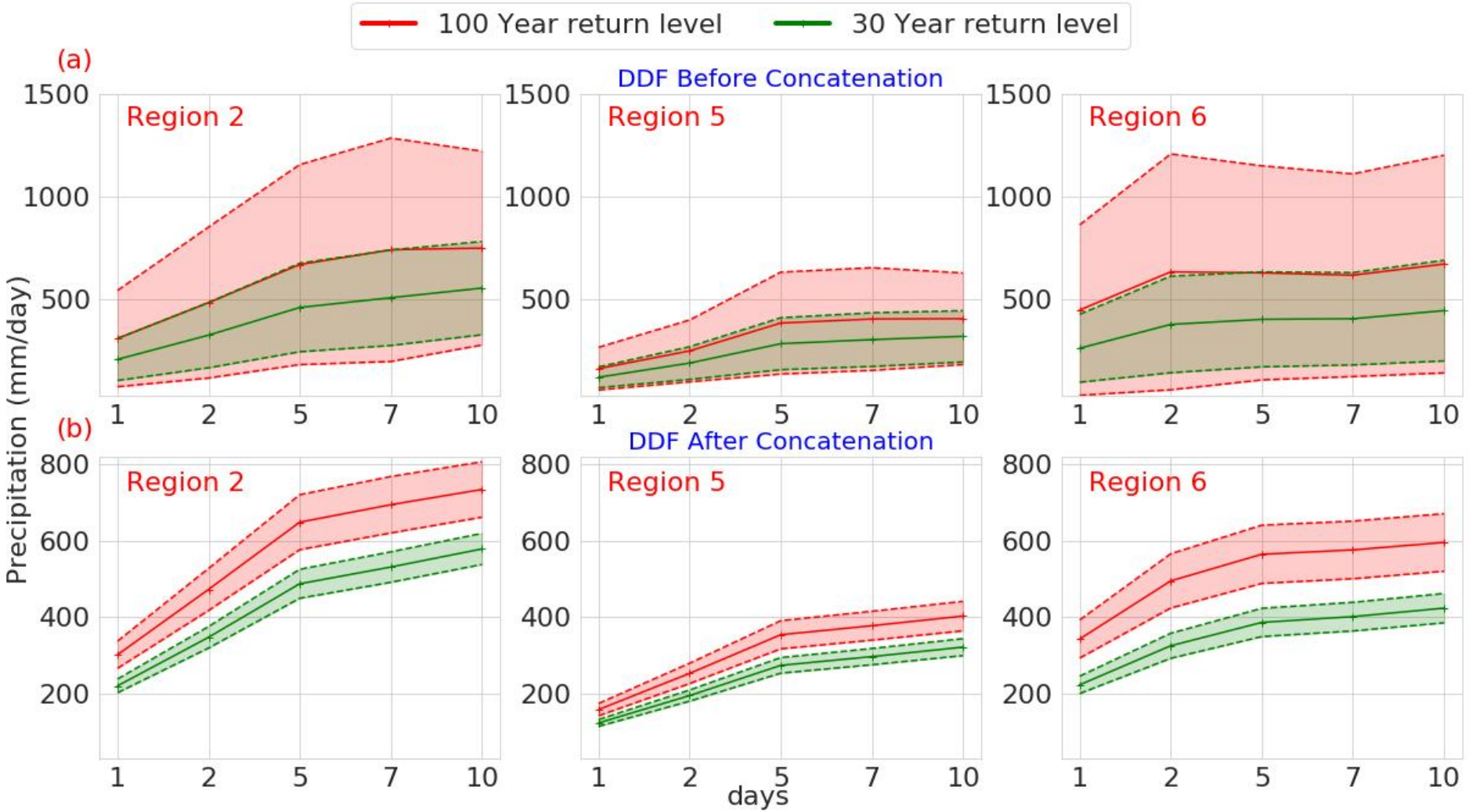
100 Year return level
30 Year return level
(a)
DDF Before Concatenation
Region 2
Region 5
Region 6
(b)
DDF After Concatenation
Region 2
Region 5
Region 6
Precipitation (mm/day)
days
1500
1000
500
800
600
400
200
1
2
5
7
10

Figure_SI3.pdf.

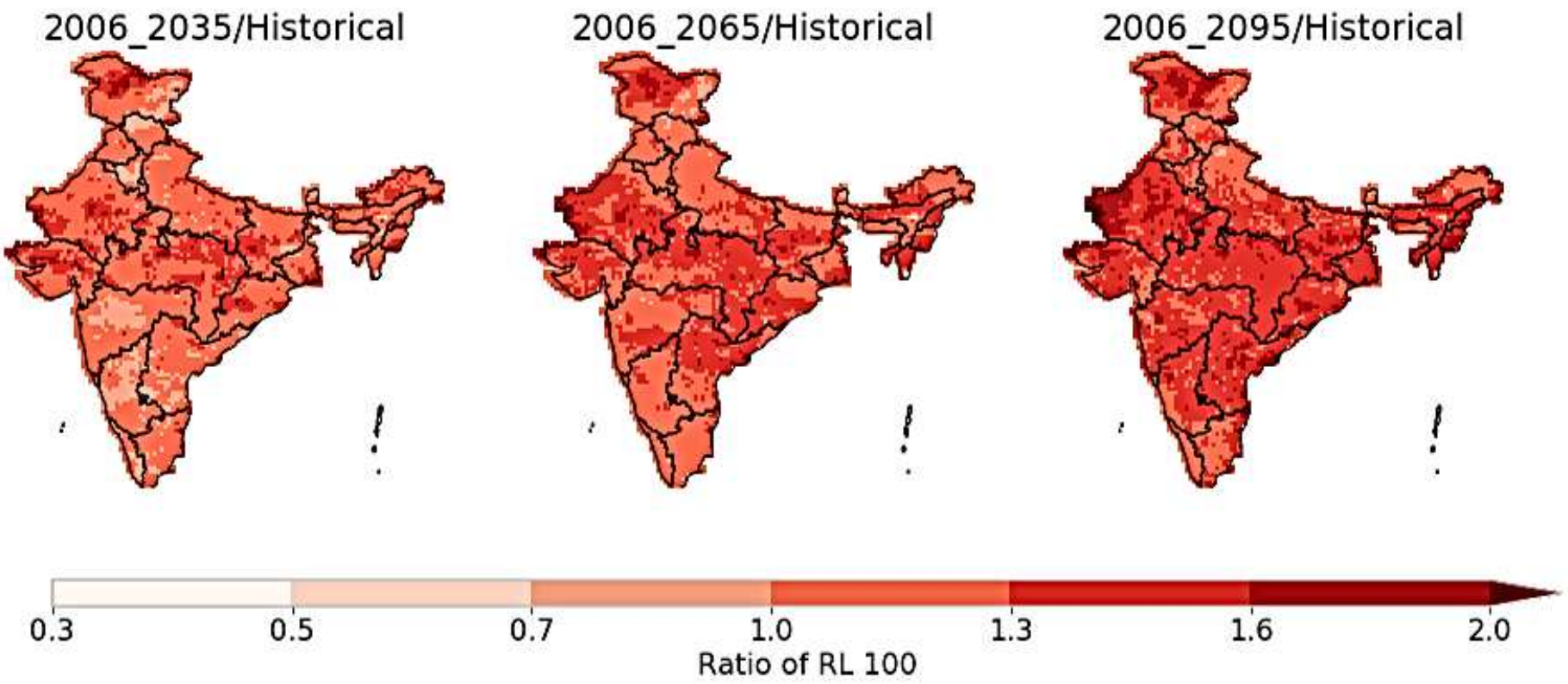
2006_2035/Historical
2006_2065/Historical
2006_2095/Historical
0.3
0.5
0.7
1.0
1.3
1.6
2.0
Ratio of RL 100